A light-stimulated synaptic transistor with synaptic plasticity and memory functions based on InGaZnOx–Al2O3 thin film structure

Li, Hua Kai; Chen, Tupei; Liu, P.; Hu, S. G.; Liu, Y.; Zhang, Qing; Lee, Pooi See

2016

Li, H. K., Chen, T., Liu, P., Hu, S. G., Liu, Y., Zhang, Q., et al. (2016). A light-stimulated synaptic transistor with synaptic plasticity and memory functions based on InGaZnOx–Al2O3 thin film structure. Journal of Applied Physics, 119(24), 244505-.

https://hdl.handle.net/10356/83557

https://doi.org/10.1063/1.4955042

A light-stimulated synaptic transistor with synaptic plasticity and memory functions based on $InGaZnO_x$–Al_2O_3 thin film structure

H. K. Li,[1] T. P. Chen,[1,a)] P. Liu,[1] S. G. Hu,[1,2] Y. Liu,[2] Q. Zhang,[1] and P. S. Lee[3]
[1]*School of Electrical and Electronic Engineering, Nanyang Technological University, Singapore 639798*
[2]*State Key Laboratory of Electronic Thin Films and Integrated Devices, University of Electronic Science and Technology of China, Chengdu, Sichuan 610054, People's Republic of China*
[3]*School of Materials Science and Engineering, Nanyang Technological University, Singapore 639798*

(Received 10 May 2016; accepted 18 June 2016; published online 29 June 2016)

In this work, a synaptic transistor based on the indium gallium zinc oxide (IGZO)–aluminum oxide (Al_2O_3) thin film structure, which uses ultraviolet (UV) light pulses as the pre-synaptic stimulus, has been demonstrated. The synaptic transistor exhibits the behavior of synaptic plasticity like the paired-pulse facilitation. In addition, it also shows the brain's memory behaviors including the transition from short-term memory to long-term memory and the Ebbinghaus forgetting curve. The synapse-like behavior and memory behaviors of the transistor are due to the trapping and detrapping processes of the holes, which are generated by the UV pulses, at the IGZO/Al_2O_3 interface and/or in the Al_2O_3 layer. *Published by AIP Publishing.*
[http://dx.doi.org/10.1063/1.4955042]

I. INTRODUCTION

A modern digital computer is based on the von Neumann' architecture,[1] in which the memory and processor are physically separated. Despite of the achievements made so far, the von Neumann architecture is becoming increasing inefficient for the further requirement for complicated computation or recognition due to the physical separation of computing parts and memories. In contrast, the human brain deals with information in parallel, enabling the brain to efficiently process information with low power consumption.[2] Therefore, many efforts have been made to build neuromorphic systems that can mimic the human brain, which is believed to be the most powerful information processor that can easily recognize various objects and visual information in complex world environment through complicated computation.[3] The human brain is composed of $\sim 10^{15}$ synapses, which have signal processing, memory, and learning functions; thus the synapse emulation is a key step to realize the neuromorphic computation.[4] Though many works have been done to implement neuromorphic systems through software-based method by conventional von Neumann computers,[5] or hardware-based methods by emulating the synapse with a large number of transistors and capacitors in complementary metal-oxide-semiconductor (CMOS) integrated circuits,[2] both of the two approaches occupy larger areas and consume much more energy than the human brain. Thus, the realization of a single device with synaptic functions has attracted much attention for the implementation of the neuromorphic system.

Nowadays, a variety of electronic synapses based on two-terminal memristors or three-terminal synaptic transistors has been demonstrated.[6–16] However, to the best of our knowledge, the reported electronic synapses were usually stimulated with electrical stimulus; and few artificial synapses based on light stimulus have been reported. Compared with the electrical stimulus, the light stimulus may offer some advantages, e.g., a much wider bandwidth and no RC delay for signal transmission. Thus, the demonstration of a synapse operated with light stimulus provides an alternative way for the emulation of biological synapse.

In this work, a light-stimulated synaptic transistor has been fabricated based on the indium gallium zinc oxide (IGZO)–aluminum oxide (Al_2O_3) thin film structure. Synaptic plasticity and memory behaviors including paired-pulse facilitation (PPF), short-term memory (STM) to long-term memory (LTM) transition, and Ebbinghaus forgetting curve were mimicked in this synaptic transistor with light stimulus.

II. EXPERIMENT

The synaptic transistor based on the IGZO–Al_2O_3 thin film structure was fabricated with the following sequence. First, a 30 nm Al_2O_3 thin film was deposited on a heavily doped *n*-type Si substrate with atomic layer deposition (ALD) process at the temperature of 250 °C. Then, a IGZO thin film with the thickness of ~50 nm was deposited onto the Al_2O_3 thin film by radio frequency (RF) magnetron sputtering of an IGZO target in a mixed Ar/O_2 ambient with the Ar partial pressure of 3×10^{-3} Torr and O_2 partial pressure of 2×10^{-4} Torr. In the device structure of the synaptic transistor shown in the inset of Fig. 1(a), the Al_2O_3 thin film, IGZO thin film, and heavily doped *n*-type Si substrate serve as the gate dielectric, channel layer, and bottom gate of the transistor, respectively. The pattern of the IGZO channel with the length of 20 μm and width of 40 μm was formed with lithography and a wet etching process. Finally, 100 nm Au/20 nm Ti layer was deposited by electron-beam evaporation at room temperature to form the source and drain electrodes of the transistor. All the characterizations were conducted in the air ambient. To avoid any additional charge trapping in the passivation layer and/or at the passivation

a)Electronic mail: echentp@ntu.edu.sg.

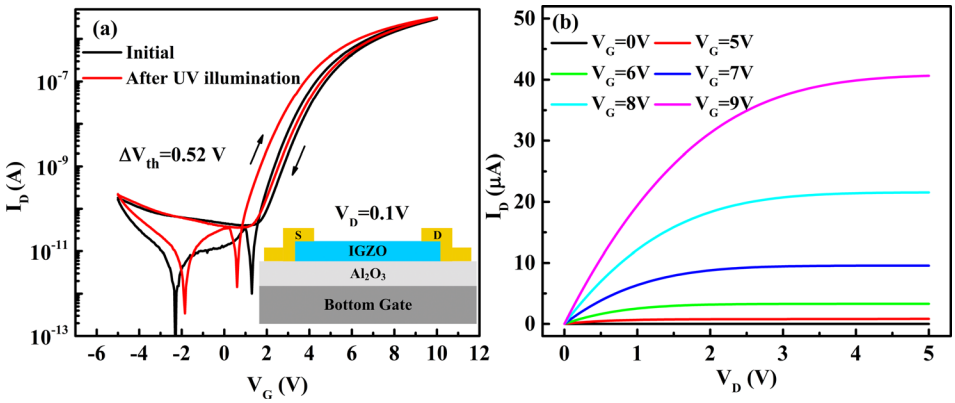

FIG. 1. (a) Transfer characteristics (I_D versus V_G) of the bottom-gate IGZO synaptic transistor at $V_D = 0.1$ V before and after 1 s UV light illumination. The inset shows the schematic cross-sectional diagram of the transistor. (b) Output characteristics (I_D versus V_D) of the bottom-gate IGZO synaptic transistor.

layer/IGZO interface caused by ultraviolet (UV) illumination, no passivation layer on the exposed IGZO surface was used in this work. Electrical characterization of the synaptic transistor was conducted with a Keithley 4200 semiconductor characterization system at room temperature. In the experiments of synaptic plasticity and memory behaviors of the synaptic transistor, the light stimulus was supplied with a UV spot light source with the wavelength of 365 nm (HAMAMATSU-LC8 spot light source). The spot of the UV illumination is a circle with the diameter of 3 mm, which is larger than the thin film transistor (TFT) channel. However, as the IGZO channel is patterned, only the device that is exposed to the UV illumination will be influenced by the light.

III. RESULTS AND DISCUSSION

We first investigated the electrical characteristics of the bottom-gate IGZO synaptic transistor. Fig. 1(a) shows the transfer characteristics of the transistor in forward sweep from −5 V to 10 V and reverse sweep from 10 V to −5 V at the drain voltage (V_D) fixed at 0.1 V. The on/off ratio of the drain current (I_D), field-effect mobility (μ), and subthreshold swing (S.S) that are obtained from the transfer curve of the forward sweep are 3×10^6, 16 cm^2/V s, and 0.29 V/dec, respectively. Before the UV illumination, a clockwise hysteresis with the threshold-voltage (V_{th}) shift of ∼0.59 V can be observed in the transfer curves in Fig. 1(a). The clockwise hysteresis could be attributed to electron trapping at or near the IGZO/Al_2O_3 interface or within the IGZO channel layer.[17–19] The typical output characteristic of an *n*-type field effect transistor is observed from the synaptic transistor as shown in Fig. 1(b). After 1 s UV light illumination, an obvious negative shift of the transfer curve can be observed in Fig. 1(a), indicating the decrease of the threshold voltage of the transistor. The negative shift of V_{th} could be attributed to either the hole trapping at the IGZO/Al_2O_3 interface and/or in the Al_2O_3 layer or the increase of the electron concentration in IGZO channel. The latter mechanism is excluded due to the little change of the resistivity of IGZO channel with different durations of UV light exposure, which was studied in our previous work.[20] Thus, the negative shift of V_{th} can be attributed to the photo-generated holes trapped at the IGZO/Al_2O_3 interface and/or in the Al_2O_3 layer.[21–23]

Fig. 2(a) shows the schematic diagram of the IGZO-based synaptic transistor, which can be used to mimic the biological synapse shown in Fig. 2(b). In the operation of the synaptic transistor, UV light pulses, which act as the pre-synaptic input, are shone onto the IGZO channel of the transistor with the gate terminal floated and the drain voltage (V_D) fixed at 0.5 V, as shown in Fig. 2(a). The drain current and the channel conductance (measured at the drain voltage V_D of 0.5 V in this work) of the transistor are analogous to the post-synaptic current and synaptic weight, respectively. The trapping and detrapping of the photo-generated holes at the IGZO/Al_2O_3 interface and/or in the Al_2O_3 layer under the stimulation of the UV pulses play a role similar to that of a neuro-transmitter in the modulation of the strength of the synaptic connection in a biological synapse.[24] As the bandgap of the IGZO thin film is ∼3.36 eV,[25] the UV light with the photon energy of 3.4 eV generates many electron-hole pairs in the IGZO channel as shown in the inset of Fig. 2(a). A photocurrent flowing between the source and the drain in the transistor is thus produced under the influence of the drain voltage, leading to an increase of the post-synaptic current. Some of the photo-generated holes are trapped at the IGZO/Al_2O_3 interface and/or in the Al_2O_3 layer and are gradually released during the off-periods of the UV light pulses. The trapped holes induce conduction electrons in the IGZO channel layer, as shown in the inset of Fig. 2(a). As a result, the post-synaptic current does not disappear immediately when the UV light illumination is turned off. Instead, a decay of the post-synaptic current is observed during the off-periods of the UV light pulses, as shown in Fig. 2(c). The decay of the post-synaptic current is analogous to the memory loss in biological system. On the other hand, as not all of the photo-generated holes are released during the off-periods of the UV light pulses, there is an accumulation of the trapped holes, leading to a continuous increase in the post-synaptic current with number of the UV light pulses, as shown in Fig. 2(c).

Synaptic plasticity is an important characteristic of biological synapses, which can be categorized into two types, short-term plasticity (STP) and long-term plasticity (LTP), based on the retention time.[7] The STP is a temporal potentiation of the synaptic connection, which lasts for a few minutes or less; the LTP is a permanent change of the synaptic connection, which lasts for a longer time from hours to years.[4] The paired-pulse facilitation (PPF), which is a form of STP, is a phenomenon in which the post-synaptic response evoked by the spike is increased when the second spike closely

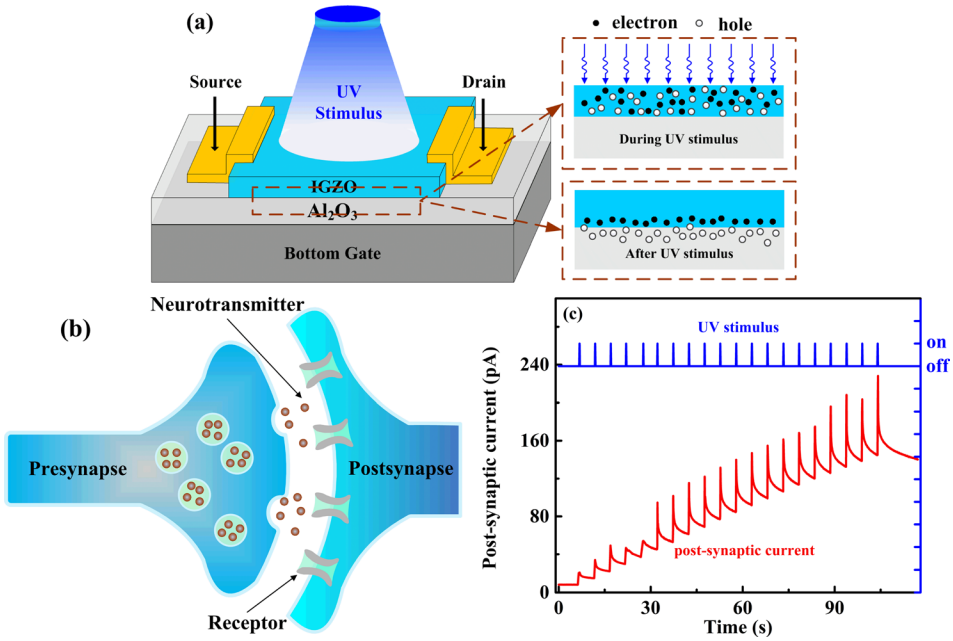

FIG. 2. Analogy between the IGZO-based synaptic transistor and a biological synapse. (a) Electron-hole pair generation in the transistor by UV stimulus and the post-stimulus distribution of the photo-generated electrons and holes. (b) Schematic illustration of a biological synapse. (c) The drain current (the post-synaptic current) of the synaptic transistor recorded in response to the UV pulse train. The intensity, width, and interval of the UV pulse train are 3 mW/cm^2, 100 ms, and 5 s, respectively; and the post-synaptic current was recorded at $V_D = 0.5$ V.

follows the previous spike.[3] The PPF is believed to play an important role in decoding temporal information in auditory or visual signals.[8] The continuous increase of the post-synaptic current with number of the UV light pulses, as shown in Fig. 2(c), provides us the possibility to mimic the PPF in our synaptic transistor with UV light stimulus. As shown in Fig. 3(a), two successive UV light pulses with fixed intensity and pulse width were applied to the IGZO channel with the pulse interval (Δt) of 2 s, and the post-synaptic current was read with V_D of 0.5 V. The post-synaptic current that triggered by the second UV light pulse is larger than the first one, which is similar to the PPF behavior in the biological synapse. The PPF of the synaptic transistor can be described with[26]

$$PPF = 100\% \cdot (A2 - A1)/A1, \tag{1}$$

where A1 and A2 are the magnitudes of the first and second post-synaptic current, respectively. The PPF decreases with the increase of the UV light pulse interval, as shown in Fig. 3(b). As illustrated in Fig. 2(a), electron-hole pairs are generated in the IGZO channel by the UV light. After the first UV light pulse, some of the photo-generated holes are trapped at the IGZO/Al_2O_3 interface and/or in the Al_2O_3 layer. If the interval is small enough, the trapped holes that are generated during the first UV light pulse will not be completely released before the second light pulse arrives. Correspondingly, the conduction electrons in the IGZO channel induced by the trapped holes will not disappear completely, and thus the post-synaptic current that triggered by the second UV light pulse is larger than the first one. With a longer pulse interval, more trapped holes are released, resulting in a smaller second post-synaptic current and thus a smaller PPF as shown in Fig. 3(b). The PPF decay with the pulse interval can be divided into a rapid phase and a slow phase, which is analogous to the PPF decay observed in a biological synapse. The PPF decay can be described as[26]

$$PPF = c_1 \cdot \exp(-\Delta t/\tau_1) + c_2 \cdot \exp(-\Delta t/\tau_2), \tag{2}$$

where Δt is the UV light pulse interval, c_1 and c_2 are the initial facilitation magnitudes of the rapid and slow phases, respectively, and τ_1 and τ_2 are the characteristic relaxation time of the rapid and slow phases, respectively. The experimental PPF decay with the UV light pulse interval is well fitted in Eq. (2), as shown in Fig. 3(b). The values of c_1, c_2, τ_1, and τ_2 yielded from the fitting are 35.9%, 35.5%, 3.1 s, and 839 s, respectively.

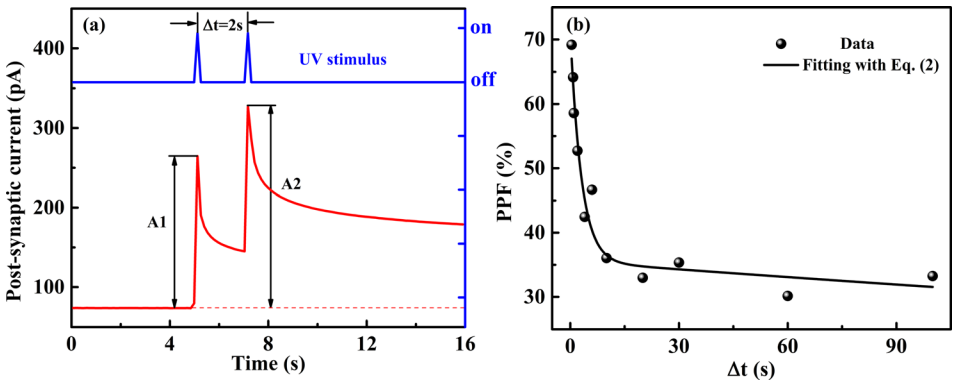

FIG. 3. (a) Post-synaptic currents of the synaptic transistor triggered by a pair of UV light pluses. The pulse intensity, pulse width, and pulse interval are 3 mW/cm^2, 100 ms, and 2 s, respectively. The post-synaptic current was measured with V_D of 0.5 V. A1 and A2 are the magnitudes of the first and second post-synaptic currents, respectively. (b) PPF decays with the pulse interval (Δt). The pulse intensity and width are fixed at 3 mW/cm^2 and 100 ms, respectively. The experimental data are the average values of the PPF obtained from 10 independent tests.

The memory behavior in psychology, which can also be categorized into short-term memory (STM) and long-term memory (LTM) based on the retention time, corresponds to the plasticity in neuroscience.[7] Thus, the synaptic transistor can also mimic the human memory by taking the UV light stimulus and channel conductance as the external stimulus and memory level, respectively. As shown in Fig. 2(c), the post-synaptic current increases after each UV light pulse; and the current decays during the interval period between two pulses. The former and latter are analogous to the enhancement of the memorization through stimulation/impression and the forgetting behavior in human brain, respectively. In the synaptic transistor, the transition from STM to LTM can be realized by repeating the UV pulse stimulus, which is analogous to the rehearsal in human daily life. To study the transition from STM to LTM in the synaptic transistor, a series of UV light pulses with fixed intensity, width, and interval (which are 3 mW/cm^2, 100 ms, and 100 ms, respectively) were applied to the IGZO channel, and the conductance was recorded with V_D of 0.5 V immediately after the last pulse of a pulse series. Fig. 4(a) shows the decays of the normalized channel conductance change recorded after the last pulse of the UV pulse series of 10, 50, and 90 pulses, respectively. The synaptic weight (i.e., the channel conductance) of the synaptic transistor decays very fast at the beginning and then slowly, which is indeed analogous to the human memory.[6] The decay of the channel conductance can be described by[27]

$$\Delta G(t)/\Delta G_0 = \exp[-(t/\tau)^{\beta}], \tag{3}$$

where $\Delta G(t) = G(t) - G_{init}$ and $\Delta G_0 = G_0 - G_{init}$, G(t) is the channel conductance at time t, G_0 is the channel conductance recorded immediately after the last pulse of a pulse series, G_{init} is the channel conductance before any UV light stimulus, τ is the characteristic relaxation time, and β is an index between 0 and 1. The decay behavior described in Eq. (3) is analogous to the well-known Ebbinghaus forgetting curve. The Ebbinghaus forgetting curve hypothesizes the decay of human memory in time. It shows how information is lost over time in human brain.[28,29] The characteristic relaxation time (τ) can be obtained from the fitting to the experimental data with Eq. (3). As shown in Fig. 4(a), the conductance decay behavior of the synaptic transistor can be well described with Eq. (3). Both the channel conductance change and characteristic relaxation time yielded from the fitting increase with the UV light pulse number, as shown in Fig. 4(b), which is analogous to the memory behavior of the human brain that repeating stimulus can strengthen the impression and decrease the forgetting rate. The increase of both the channel conductance and characteristic relaxation time is the strong evidence for the transition from STM to LTM.[4] Besides the pulse number, the pulse width also has an effect on the memory strength and forgetting rate, which is demonstrated by the result shown in Fig. 4(c). In the experiment of Fig. 4(c), 20 successive UV light pulses with fixed intensity (3 mW/cm^2) and pulse interval (100 ms) but varied pulse width were applied to the IGZO channel. Both the channel conductance and characteristic relaxation time increase with the pulse width, indicating that the transition from STM to LTM can also be realized by increasing the UV light pulse width.

IV. CONCLUSIONS

In conclusion, an UV pulse-stimulated synaptic transistor based on the IGZO–Al_2O_3 thin film structure has been demonstrated. The synaptic transistor exhibits the behaviors of synaptic plasticity like the paired-pulse facilitation. In addition, the brain's memory behaviors including the

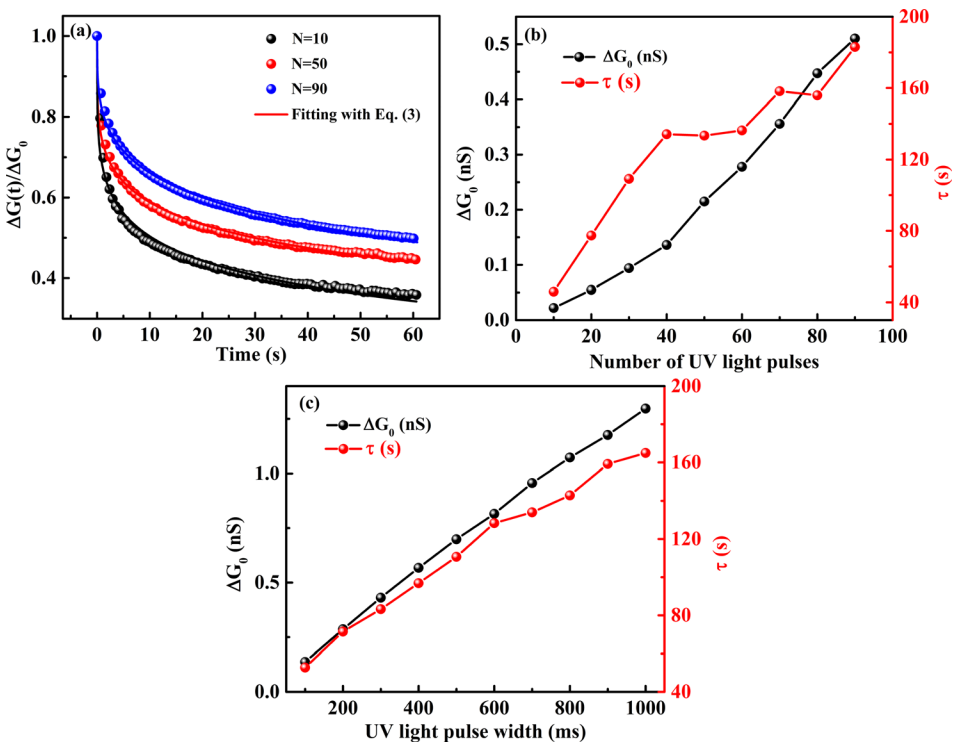

FIG. 4. (a) Decay of the normalized channel conductance change recorded after the last pulse of an UV pulse series for various pulse numbers (N). The pulse intensity, pulse width, and pulse interval are 3 mW/cm^2, 100 ms, and 100 ms, respectively. The lines are the best fittings to the experimental data with Eq. (3). (b) ΔG_0 and τ yielded from the fittings in (a) as a function of the UV light pulse number. (c) ΔG_0 and τ as a function of the UV light pulse width. In the experiment of (c), 20 successive UV light pulses with the intensity of 3 mW/cm^2 and pulse interval of 100 ms were applied to the synaptic transistor.

transition from short-term memory to long-term memory and the Ebbinghaus forgetting curve can be also mimicked with the synaptic transistor. The synapse-like behaviors and memory behaviors of the synaptic transistor are due to the trapping and detrapping of the photo-generated holes at the IGZO/Al_2O_3 interface and/or in the Al_2O_3 layer.

ACKNOWLEDGMENTS

This work was financially supported by the National Research Foundation of Singapore (Program Grant No. NRF-CRP13-2014-02), MOE Tier 2 (Program Grant No. MOE 2013-T2-2-100/ARC 24/14), and NTU-A*STAR COE-Si (Program Grant No. 112 3510 0003). Y. Liu would like to acknowledge the support by NSFC under Project No. 61274086.

[1]J. Von Neumann, Ann. Hist. Comput. **10**, 243 (1988).
[2]R. Yang, K. Terabe, Y. Yao, T. Tsuruoka, T. Hasegawa, J. K. Gimzewski, and M. Aono, Nanotechnology **24**, 384003 (2013).
[3]L. Q. Zhu, C. J. Wan, L. Q. Guo, Y. Shi, and Q. Wan, Nat. Commun. **5**, 3158 (2014).
[4]S. Z. Li, F. Zeng, C. Chen, H. Y. Liu, G. S. Tang, S. Gao, C. Song, Y. S. Lin, F. Pan, and D. Guo, J. Mater. Chem. C **1**, 5292 (2013).
[5]S. Furber, IEEE Spectrum **49**, 44 (2012).
[6]T. Chang, S. H. Jo, and W. Lu, ACS Nano **5**, 7669 (2011).
[7]Z. Q. Wang, H. Y. Xu, X. H. Li, H. Yu, Y. C. Liu, and X. J. Zhu, Adv. Funct. Mater. **22**, 2759 (2012).
[8]K. Kim, C. L. Chen, Q. Truong, A. M. Shen, and Y. Chen, Adv. Mater. **25**, 1693 (2013).
[9]S. H. Jo, T. Chang, I. Ebong, B. B. Bhadviya, P. Mazumder, and W. Lu, Nano Lett. **10**, 1297 (2010).
[10]L. Chen, C. Li, T. Huang, H. G. Ahmad, and Y. Chen, Phys. Lett. A **377**, 3260 (2013).
[11]J. D. Greenlee, C. F. Petersburg, W. Laws Calley, C. Jaye, D. a. Fischer, F. M. Alamgir, and W. Alan Doolittle, Appl. Phys. Lett. **100**, 182106 (2012).
[12]J. Hermiz, T. Chang, C. Du, and W. Lu, Appl. Phys. Lett. **102**, 083106 (2013).
[13]S. Pinto, R. Krishna, C. Dias, G. Pimentel, G. N. P. Oliveira, J. M. Teixeira, P. Aguiar, E. Titus, J. Gracio, J. Ventura, and J. P. Araujo, Appl. Phys. Lett. **101**, 063104 (2012).
[14]S. G. Hu, Y. Liu, Z. Liu, T. P. Chen, Q. Yu, L. J. Deng, Y. Yin, and S. Hosaka, J. Appl. Phys. **116**, 214502 (2014).
[15]C. J. Wan, L. Q. Zhu, J. M. Zhou, Y. Shi, and Q. Wan, Nanoscale **5**, 10194 (2013).
[16]C. J. Wan, L. Q. Zhu, J. M. Zhou, Y. Shi, and Q. Wan, Nanoscale **6**, 4491 (2014).
[17]K. Hoshino, D. Hong, H. Q. Chiang, and J. F. Wager, IEEE Trans. Electron Devices **56**, 1365 (2009).
[18]J. Triska, J. F. Conley, R. Presley, and J. F. Wager, J. Vac. Sci. Technol., B **28**(4), C5I1 (2010).
[19]J. F. Wager, D. A. Keszler, and R. E. Presley, *Transparent Electronics* (Springer, New York, 2008).
[20]P. Liu, T. P. Chen, X. D. Li, Z. Liu, J. I. Wong, Y. Liu, and K. C. Leong, Appl. Phys. Lett. **103**, 202110 (2013).
[21]K. H. Ji, J. I. Kim, Y. G. Mo, J. H. Jeong, S. Yang, C. S. Hwang, S. H. K. Park, M. K. Ryu, S. Y. Lee, and J. K. Jeong, IEEE Electron Device Lett. **31**, 1404 (2010).
[22]K. H. Lee, J. S. Jung, K. S. Son, J. S. Park, T. S. Kim, R. Choi, J. K. Jeong, J. Y. Kwon, B. Koo, and S. Lee, Appl. Phys. Lett. **95**, 232106 (2009).
[23]J.-Y. Kwon, K. S. Son, J. S. Jung, K. H. Lee, J. S. Park, T. S. Kim, K. H. Ji, R. Choi, J. K. Jeong, B. Koo, and S. Lee, Electrochem. Solid-State Lett. **13**, H213 (2010).
[24]T. Hasegawa, K. Terabe, T. Tsuruoka, and M. Aono, Adv. Mater. **24**, 252 (2012).
[25]X. D. Li, S. Chen, T. P. Chen, and Y. Liu, ECS Solid State Lett. **4**, P29 (2015).
[26]S. G. Hu, Y. Liu, T. P. Chen, Z. Liu, Q. Yu, L. J. Deng, Y. Yin, and S. Hosaka, Appl. Phys. Lett. **102**, 183510 (2013).
[27]S. G. Hu, Y. Liu, T. P. Chen, Z. Liu, Q. Yu, L. J. Deng, Y. Yin, and S. Hosaka, Appl. Phys. Lett. **103**, 133701 (2013).
[28]H. Ebbinghaus, *Translation of Memory: A Contribution to Experimental Psychology* (Dover Publications, New York, 1987).
[29]D. C. Rubin, S. Hinton, and A. Wenzel, J. Exp. Psychol. Learn. Mem. Cogn. **25**, 1161 (1999).